Characterization of nanocrystalline $(Th_{1-x}Ce_x)O_y$ powders synthesized by co-precipitation process ☆

Ö. Yildiz

Kocaeli University, Faculty of Engineering, Department of Metallurgical and Materials Engineering, Veziroglu Yerleskesi, 41040 Kocaeli, Turkey

Abstract

Nanocrystalline thoria–ceria $(Th_{1-x}Ce_x)O_y$ powders in a ratio of $x = 0.05 - 0.5$ mol% were prepared by a co-precipitation process, which employs thorium and cerium nitrate as thorium and cerium source material, deionized water as solvent and ammonia gas as precipitant. Cerium was used as a simulator for plutonium and the other actinides with a +4 valency. After co-precipitation the aqueous $(Th_{1-x}Ce_x)(OH)_y \cdot nH_2O$ cakes had been dried at 110 °C, these powders were separately milled in acetone, carbon tetrachloride, n-dodecane, isopropanol and water before and/or after calcination at different temperatures (300–600 °C). DTA-TG, XRD, TEM and BET analyses were performed to characterize the produced powders. Characterization results revealed that the materials were not crystallized, even the temperature reached up to 600 °C. The crystallization of $(Th_{1-x}Ce_x)O_y$ began at about 600 °C. The crystal growth took place between the temperatures 600 °C and 1200 °C. The powders have a range average crystallite sizes from 5 to 115 nm, with a specific surface area from 6 to 111 m²/g depending on the calcination temperature and Ce mol%. In this way the crystallized nano $(Th_{1-x}Ce_x)O_2$ powder with a higher specific surface area is able to be produced to obtain the pellets in very high density.

© 2007 Elsevier B.V. All rights reserved.

1. Introduction

The minor actinides especially Pu, Np and Am, which occur as decay products in nuclear reactors, are the most important nuclides determining the long-time risk of final disposal. Therefore after separation from the fission products the minor actini-des must be deposited of in a safe environment or they must be further processed as fuel.

Various investigations for many kinds of materials, ceramic as the most important of them well-known for its characteristic properties, have been already realized for the final disposal of plutonium and the other minor actinides both excess from dismantled nuclear weapons. Some of these studies concerning different types of ceramic materials can be found in literature [1–5].

Thorium dioxide ceramic is an important material for immobilizing of tetravalent long-lived actinides and transmutation of fission products, due to

its interesting properties. Crystallized thoria is known to be very insoluble in aqueous media [6]. Thoria has a face-centered cubic (fcc) fluorite-type crystal structure that is isomorphic with that of tetravalent actinides dioxides (UO_2, PuO_2 and NpO_2) [7,8]. There has been a considerable interest in studying the feasibility of thorium-based fuel reactors, in order to decrease production of radionuclides and especially that of minor actinides and plutonium [9]. As a matter of fact ThO_2 is an important refractory material with a high fusion temperature (3360 °C) for high temperature application and exhibits a good resistance to irradiation [7,8].

CeO_2 has been used as a surrogate material to simulate of PuO_2 or the other actinides with a +4 valency [10–12]. ThO_2 and CeO_2 form almost an ideal solid solution in the complete homogeneity and composition range [10–13]. CeO_2 and PuO_2 have quite similar physico-chemical properties, namely, ionic sizes in octahedral and cubic coordination, melting points, standard enthalpy of formation and specific heat. The dissolution behaviour of them into the crystalline assemblage are generally coincided and the overall shrinkage under the baseline sintering conditions is essentially identical. Thus the plutonium chemistry can be well simulated using CeO_2 in place of highly active PuO_2 [12,14,15]. The thermo-physical properties, the bulk and lattice thermal expansion behaviour of thorium-based systems with PuO_2 and the oxides of the some fission products have been investigated by several groups [10,11,16,17]. Tyagi and Mathews [16] have used CeO_2 as a surrogate material in place of PuO_2 to simulate the thermal expansion behavior of $Th_{1-x}Pu_xO_2$ ($x = 0.04$ and 0.08). In this perspective, they have also studied the bulk thermal expansion behaviour and thermodynamic properties of $Th_{1-x}Ce_xO_2$ in the complete solid solution range [16,17].

There are many ways to synthesize the mixed oxide powders of $(Th_{1-x}Ce_x)O_y$. Sol–gel, co-precipitation and thermal treatment (heating of precursor materials) are well-known production methods. Haas [18] has produced thoria powdered samples by converting a thorium nitrate solution into a sinterable powder using a sol–gel process. Whitfield et al. [19] have prepared two series of mixed oxides of $(ThCe)O_2$ and $(ThCe)O_{2-x}$ by hydrogen reduction in the temperature range of 973–1673 K. Thoria–ceria ceramic materials, in which ThO_2 powder was blended with $(Th_{0.87}Ce_{0.13})O_2$ coprecipitated powder, have been produced to get the sintered pel-

lets with the mean composition of $(Th_{0.94}Ce_{0.06})O_2$ [20]. Crystallized thoria powder have been obtained also by heating various precursors such as thorium nitrate, oxalate or hydroxide at various temperatures ranging from 700 °C up to 1600 °C [21,22]. Hubert et al. [7] have prepared ThO_2 powder by heat treatment of thorium oxalate and by precipitation of hydroxide to study the influence of the precursor and the calcination temperature on the dissolution of thorium dioxide.

In this work, the nanocrystalline $(Th_{1-x}Ce_x)O_y$ powders were synthesized and characterized to finally dispose of the minor actinides (Pu and the other with a +4 valence) as a stable solid solution in ThO_2-based ceramic materials. In the experimental studies, co-precipitation method was used to synthesize the nanocrystalline $(Th_{1-x}Ce_x)O_y$ powders, utilizing cerium as a simulator for these actinides. The powder characteristics like decomposition, crystallization, crystallite size and specific surface area were investigated depending on the ratio of Ce (5–50 mol%), the calcination temperature and the grinding solution.

2. Experimental procedures

2.1. Chemicals

$Th(NO_3)_4 \cdot 5H_2O$ with a purity of 99 wt% from Merck and $Ce(NO_3)_3 \cdot 6H_2O$ with a purity of 99.5 wt% from Alfa Aesar, ammonia gas (99.98%) as a precipitator and distilled water as a solvent were used to prepare $(Th_{1-x}Ce_x)(OH)_y$ powders.

2.2. Preparation of $(Th_{1-x}Ce_x)O_y$ powders

Precipitation process was performed on a magnetic stirrer at the room temperature. $Th(NO_3)_4 \cdot 5H_2O$ and $Ce(NO_3)_3 \cdot 6H_2O$ were dissolved in distilled water in a ratio of Ce (5–50 mol%). During the mixing of nitrate solution, ammonia gas was given slowly in a maximum flow rate of 6 l/min. The precipitates were formed in 20 min for 2.5 l solution. The samples were filtered by a suction funnel filter with the help of vacuum pump, washed several times simultaneously with distilled water and dried for 3 days at 110 °C in dryer furnace. After than $(Th_{1-x}Ce_x)(OH)_y$ powders were calcined at different temperatures (300, 420 and 600 °C) before and/or after grinding of the powder materials.

2.3. Powder characterization

The dried and calcined powders were characterized before and after calcinations using several techniques. Differential thermal analysis with thermogravimeter (DTA-TG), X-ray powder diffraction (XRD) and transmission electron microscope (TEM) were used to examine crystallization and morphology. The specific surface area of powders was determined by using BET method.

In order to determine the thermal behaviour of powders during heating ranging from room temperature to 1400 °C, differential thermal analysis (DTA) and thermogravimetric analysis (TG) were carried out by using a DTA-TG system, Model STA 449C from NETZSCH with a heating rate of 5 K/min in air.

XRD was used to observe the crystal structure and the influence of the temperature on the crystallization. The X-ray diffraction patterns were recorded on a STOE & Cie STADI P Diffractometer using Co–$K_{\alpha 1}$ radiation with characteristic wavelength $\lambda = 1.78897$ Å ($2\theta = 5$–$85°$) at room temperature.

TEM was used to examine the crystallization, morphology and grain sizes of the calcined and grinded powders. The diffraction pattern and TEM images were taken with an instrument from Philips CM30 type at 'Institut für Gesteinshüttenkunde der RWTH Aachen'.

The specific surface area was measured with a Quantasorb type apparatus from Quanta Chrome using the BET method (adsorption of nitrogen). The powders were prepared from the calcined and uncalcined hydroxide and the samples were dried at 120 °C for 3 h, and than measurements were carried out. Here, the influences of heat treatment on the specific surface area of powders were studied.

3. Results and discussion

After dried, the Th(OH)$_4$ sample had a white colour and the other (Th$_{1-x}$Ce$_x$)(OH)$_y$ samples had a yellowish colour. That was dependent on the weight percentage of cerium in mixing. In other words the cerium oxide has a yellow colour if cerium oxide is in a CeO$_2$ form. Therefore, the precipitates can be called as (Th$_{1-x}$Ce$_x$)(OH)$_4$.

3.1. Thermal behaviour of the (Th$_{1-x}$Ce$_x$)(OH)$_4$ powders

The thermal behaviour of the dried (Th$_{1-x}$Ce$_x$)(OH)$_4$ powders were characterized by differential thermal analysis with thermogravimeter (DTA-TG). According to the DTA-TG analysis, draining began at ~110 °C in all samples and the mass loss continued until ~600 °C (Figs. 1 and 2). During heating of the samples from 110 to 600 °C a mass loss ca. 8 wt% was revealed; but, after 600 °C no significant mass loss was observed. Among all samples Th(OH)$_4$ had the highest mass loss (Fig. 2), while the (Th$_{0.85}$Ce$_{0.15}$) (OH)$_4$ sample had a lowest mass loss, although the (Th$_{1-x}$Ce$_x$)(OH)$_4$ samples had a similar TG-curve.

Ranging from 150 to 800 °C, there were two main temperature fields (150–300 °C and 400–500 °C), where the highest mass loss and endothermic reactions were arisen. One exothermic peak was expected to occur at 350–400 °C for CeO$_2$ [23] and the crystallization of ThO$_2$ to take place about 700 °C [24]. However, as seen from the Fig. 2, this did not turn out and the nested complex endothermic and exothermic effects could not be clearly
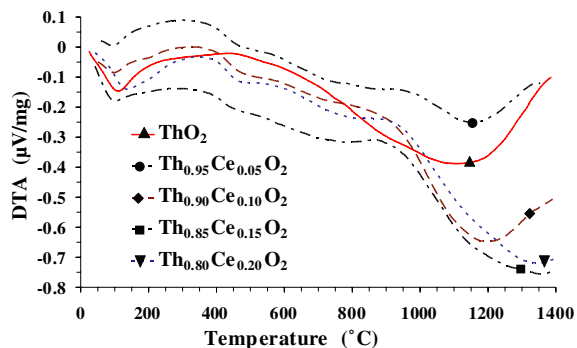

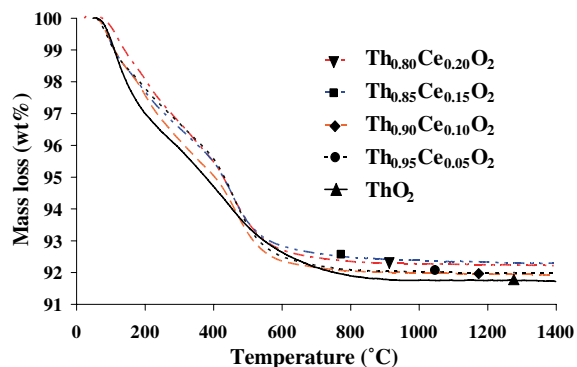Fig. 1. DTA-TG analysis of Th(OH)$_4$ and (Th$_{1-x}$Ce$_x$)(OH)$_4$ powder materials ($x = 0.05$–0.20).

Fig. 2. Thermogravimetric analysis of Th(OH)$_4$ and (Th$_{1-x}$Ce$_x$)(OH)$_4$ powder materials ($x = 0.05$–0.20).
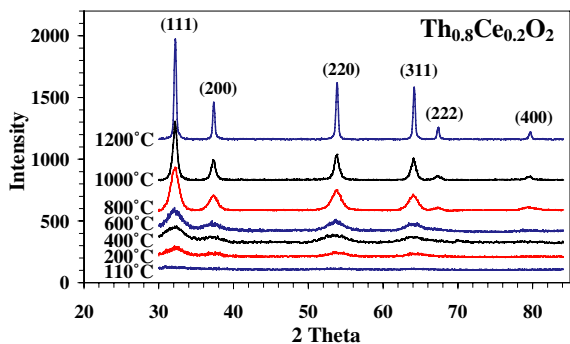
Fig. 3. XRD analysis of $(Th_{0,8}Ce_{0,2})(OH)_4$ powder materials heated at different temperatures.
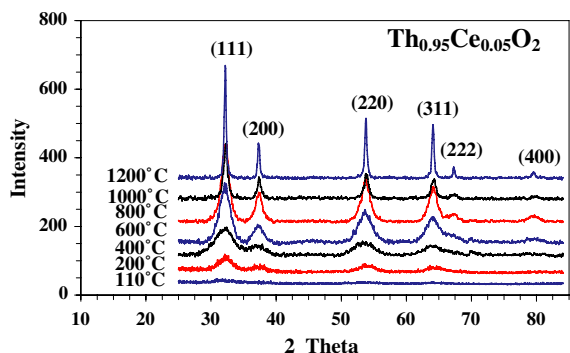

Fig. 4. XRD analysis of $(Th_{0.95}Ce_{0.05})(OH)_4$ powder materials heated at different temperatures.

identified. Since ThO_2's and CeO_2's endothermic and exothermic peaks mutually affect each other.

The influence of temperature and mol% of Ce on the crystallization of mixture can be better identified by XRD analysis (Figs. 3 and 4) than DTA. The samples with more mol% of Ce have a stronger intensity of the XRD peaks than those of the other samples with less mol% of Ce. The influence of this effect in mixture was shown in Fig. 3. The sharpness of the XRD peaks was identified in the samples heated at high temperatures (>800 °C) (Fig. 3). All the powder materials were crystallized at 100 percent at about 1200 °C (Figs. 3 and 4). The influence of heat treatment on the crystallization can be revealed in electron diffraction patterns using TEM as well (Fig. 5).

3.2. Physical behaviour of the $(Th_{1-x}Ce_x)(OH)_4$ powders

According to the DTA-TG analysis, the powder samples were calcined at different temperatures

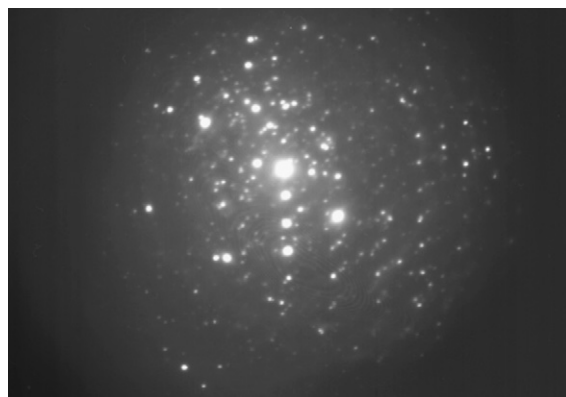Fig. 5. Electron diffraction pattern obtained using TEM from $(Th_{0.95}Ce_{0.05})O_2$ powders heated at 1200 °C.

(300–600 °C) before and/or after grinding. The grinding of one sample was realized in different solvents (acetone, carbon tetrachloride, n-dodecane, isopropanol and water) to compare the influence of the grinding solution on the specific surface area of powders. As shown in Fig. 6, all of these solvents, acetone is the best to grind of these powder materials. Carbon tetrachloride and acetone have similar effects on the specific surface area but carbon tetrachloride has a higher evaporation temperature and higher toxicity than those of acetone. Furthermore, carbon tetrachloride has a carcinogenic characteristic and the recycling of acetone is easer than that of carbon tetrachloride.

Therefore the powder materials were grinded in a ball mill for 6 h using Al_2O_3 ball in acetone solution to investigate the influence of mol% of Ce in mixture on the specific surface area of powder materials. The results showed that as the Ce mol% increased, the specific surface area of powder materials decreased
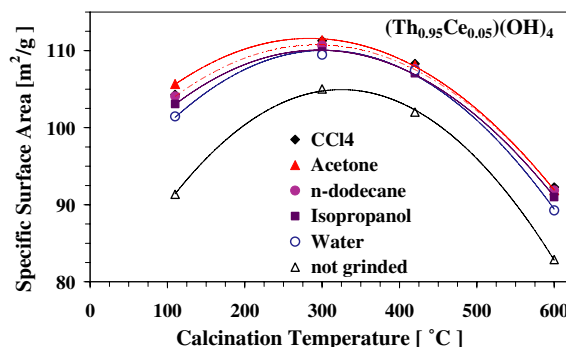

Fig. 6. The influence of the calcination temperature and grinding solution on the specific surface area of the $(Th_{0.95}Ce_{0.05})(OH)_4$ powders.
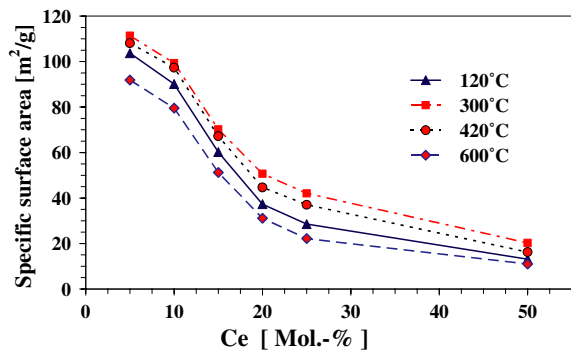
Fig. 7. The influence of CeO_2 content on the specific surface area of the $(Th_{1-x}Ce_x)(OH)_4$ powders grinded in acetone.

(Fig. 7). When the Ce mol% is risen from 20 to 50, it caused much slower decrease in the specific surface area than that of between 5 and 20. The specific surface area of $(Th_{1-x}Ce_x)(OH)_4$ was positively influenced by the heat treatment approximately until 300 °C, and it declined after 300 °C (Figs. 6 and 7).

The average crystallite sizes of these $(Th_{1-x}Ce_x)(OH)_4$ powders ranging from 5 to 115 nm were calculated from specific surface area (6–111 m^2/g in Fig. 7) depending on the content of cerium in mixture and on the calcination temperature. The TEM picture showed the morphology and crystallite size of the $(Th_{0.95}Ce_{0.05})O_2$ nanoparticles (agglomerate powders) heated at 1200 °C (Fig. 8).

The effects of grinding solution, calcining temperature and Ce mol% on the microstructure, particle size and specific surface area of powders were easily adjusted in the preparation of powder materials (Figs. 3, 4, 6 and 7). The grinding solutions (ace-
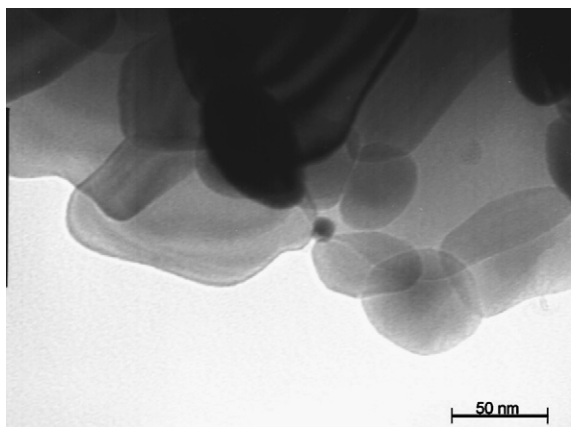
tone, carbon tetrachloride, n-dodecane, isopropanol and water) had some different effects on the property of powder materials depending on the calcining temperature (Figs. 6 and 7). Although the calcination had a positive influence on the specific surface area until 300 °C, the specific surface area of powder materials went down by calcining at high temperatures (>300 °C) (Figs. 6 and 7). Therefore, the calcination of $(Th_{1-x}Ce_x)(OH)_4$ powders at high temperatures was not appropriate to produce the ultra fine powder materials. In addition, the impurity arose from grinding ball by distribution of agglomerate in powder, when the powder was calcined at high temperatures (>300 °C especially >600 °C). When the powders were first grinded after calcined at 300 °C (or < 300 °C) and then calcined between 600 and 800 °C, these powders had the best property (high specific surface area, low particle size and good particle size distribution) for compaction. Thus, the determination of the suitable calcination temperature before grinding was very crucial. The experimental work showed that any chances in the preparation parameters of powders (precipitation, drying, calcining and grinding conditions) had a great influence on the powder characteristics. Hence, the powders with desired characteristic can be easily produced and used for all purpose by some little change or modification of these parameters.

4. Conclusions

Nanocrystalline $(Th_{1-x}Ce_x)O_2$ powders were easily synthesized using co-precipitation process. The produced powders had a property such as high specific surface area, low particle size and suitable particle size distribution for compaction. It is well known that the crystallite size (the dimension of specific surface area), especially the particle size distributions and agglomerate form of powders are very important for the compactibility. In this work it was brought about that the heat treatment of powders had a linear relation with the specific surface area until 300 °C. But, the specific surface area of powders was gone down by calcining at high temperatures (>300 °C). When the powders were calcined at high temperatures (>600 °C), the grinding of powders was problematic because the heat treatment at high temperatures led to occur the hardened agglomerate, giving rise to arising the impurities from grinding ball. According to the TG analyses, the mass losses in hydroxide powders were continued until ca. 800 °C. Therefore, the heat treatment

Fig. 8. TEM image of $(Th_{0.95}Ce_{0.05})O_2$ powder materials (agglomerate) heated at 1200 °C.

of powders must be performed before grinding at 300 °C (max. 500 °C) and after grinding at 600 °C (max. 800 °C). Among the solvents used in this work, acetone was the most suitable for grinding of powders. Given those aforementioned results, the produced powders had a high specific surface area (6–111 m^2/g) depending on the ratio of Ce (5–50 mol%) to obtain the pellets in very high density. The compactibility and sintering behaviour of nanocrystalline $(Th_{1-x}Ce_x)O_2$ powders will be presented for future work.

Acknowledgements

References

[1] W.L. Gong, W. Lutze, R.C. Ewing, J. Nucl. Mater. 277 (2000) 239.

[2] N. Dacheux, R. Podor, B. Chassigneux, V. Brandel, M. Genet, J. Alloys Comp. 271 (1998) 236.

[3] P. Taylor, W.H. Hocking, L.H. Johnson, R.J. McEacher, S. Sunder, Nucl. Technol. 116 (1996) 222.

[4] W. Lutze, R.C. Ewing, Radioactive Waste Forms for the Future, 8, Elsevier, Amsterdam, 1988, p. 495.

[5] E. Zimmer, C. Ganguly, J. Borchardt, H. Langen, J. Nucl. Mater. 152 (1988) 169.

[6] C.F. Baes, R.E. Mesmer, The Hydrolysis of Cations, Wiley Interscience, New York, 1976, p. 129.

[7] S. Hubert, K. Barthelet, B. Fourest, G. Lagarde, N. Dacheux, N. Baglan, J. Nucl. Mater. 297 (2001) 206.

[8] S. Hubert, G. Heisbourg, N. Dacheux, J. Ritt, in: 7th IMF, Petten 25–26 october, 2001.

[9] Thorium as a waste management option, Final Report of European Contract, No. FI4I/CT95-011, 1999.

[10] M.D. Mathews, B.R. Ambekar, A.K. Tyagi, J. Nucl. Mater. 288 (2001) 83.

[11] M.D. Mathews, B.R. Ambekar, A.K. Tyagi, J. Nucl. Mater. 280 (2000) 246.

[12] Y.W. Lee, H.S. Kim, S.H. Kim, C.Y. Young, S.H. Na, G. Ledergerber, P. Heimgarbner, M. Pouchon, M. Burghartz, J. Nucl. Mater. 274 (1999) 7.

[13] M.D. Freshley, H.M. Mattys, General Electric Report HW-76559, 1962, p. 11.6.

[14] J.C. Marra, A.D. Cozzi, R.A. Pierce, J.M. Pareizs, A.R. Jurgensen, D.M. Missimer, Cerium as a Surrogate in the Plutonium Immobilized Form, in WSRC-MS-2001-00007, Contract No. DE-AC09-96SR18500.

[15] C. Ganguly, in: I.J. Hasting (Ed.), Second International Conference on CANDU Fuel, Pembroke, Ont., Canada, 1989, p. 398.

[16] A.K. Tyagi, M.D. Mathews, J. Nucl. Mater. 278 (2000) 123.

[17] R.D. Purohit, A.K. Tyagi, M.D. Mathews, S. Saha, J. Nucl. Mater. 280 (2000) 123.

[18] P.A. Haas, Oak Ridge National Laboratory Report ORNL-TN-3978, 1972.

[19] H.J. Whitfield, D. Roman, A.R. Palmer, J. Inorg. Nucl. Chem. 28 (1966) 2817.

[20] A.M. Santos, F. Neto, A. Ricardo, F.S. Lameiras, P.E. Cardoso, An. Congr. Bras. Ceram. 34 (1990) 296, Pub. Assoc. Bras. Ceram., Sao Paulo, Brazil.

[21] B.J.F. Palmer, J.A. Scoberg, A.Y.H. Hin, Ceram. Bull. 62 (1982) 627.

[22] B.J.F. Palmer, L.E. Bahen, A.Y.H. Gin, J.E. Winegar, A. Celli, J. Phys. 47 (1986) C1.

[23] H.J. Choi1, J. Moon, H.B. Shim1, K.S. Han, E.G. Lee, K.D. Jung, J. Am. Ceram. Soc. 89 (2006) 343.

[24] Gmelin handbook of inorganic chemistry; Thoria, System-Nr. 44, Supplement, Springer Verlag, 1982.